

COMPRESSION OF HYPERSPECTRAL IMAGERY VIA LINEAR PREDICTION

Francesco Rizzo, Bruno Carpentieri

Dipartimento di Informatica ed Applicazioni "R.M. Capocelli", Università degli Studi di Salerno, Via S. Allende, Baronissi (SA), Italy

Giovanni Motta, James A. Storer

Computer Science Department, Brandeis University, Waltham 02454 MA, USA

Keywords: Predictive Coding, Data Compression, Remote Sensing, 3D Data.

Abstract: (Motta et al., 2003) proposed a Locally Optimal Vector Quantizer (LPVQ) for lossless encoding of hyperspectral data, in particular, Airborne Visible/Infrared Imaging Spectrometer (AVIRIS) images. In this paper we first show how it is possible to improve the baseline LPVQ algorithm via linear prediction techniques, band reordering and least squares optimization. Then, we use this knowledge to devise a new lossless compression method for AVIRIS images. This method is based on a low complexity, linear prediction approach that exploits the linear nature of the correlation existing between adjacent bands. A simple heuristic is used to detect contexts in which such prediction is likely to perform poorly, thus improving overall compression and requiring only marginal extra storage space. A context modeling mechanism coupled with a one band look ahead capability allows the proposed algorithm to match LPVQ compression performances at a fraction of its space and time requirements. This makes the proposed method suitable to applications where limited hardware is a key requirement, spacecraft on board implementation. We also present a least squares optimized linear prediction for AVIRIS images which, to the best of our knowledge, outperforms any other method published so far.

1 INTRODUCTION

In the last three decades, air-borne and space-borne remote acquisition of high definition electro-optic images has been increasingly used in military and civilian applications to recognize objects and classify materials on the earth's surface. By analyzing the spectrum of the reflected light it is possible to recognize the material(s) composing the observed scene. The development of new detector technologies has made possible the introduction of new classes of aircraft spectrometers capable of recording a large number of spectral bands over the visible and reflected infrared region. For this reason the data sets they produce are often referred to as hyperspectral. These instruments have reached spectral resolution sufficient to allow very accurate characterization of the spectral reflectance curve of a given spatial area. For example, images acquired with the JPL's Airborne Visible/Infrared Imaging

Spectrometer, AVIRIS (NASA, 2003), have pixels covering an area of approximately 20x20 meters, with radiance decomposed into 224 narrow bands, approximately 10nm wide each, in the range 400-2,500nm. Spectral components are represented with a 16 bits precision.

Hyperspectral imagery is a rapidly growing source of remote sensed data, even though its precision pales compared to the millions of channels of a truly high resolution lab spectrometer. The technology seems mature enough to use higher resolution, space-borne spectrometers. In fact, increasing the number of bands, i.e. the spectral resolution, allows for more sophisticated analysis and increases the data rate by only a linear amount. The problem is that the acquisition of these images already produces large amounts of highly correlated

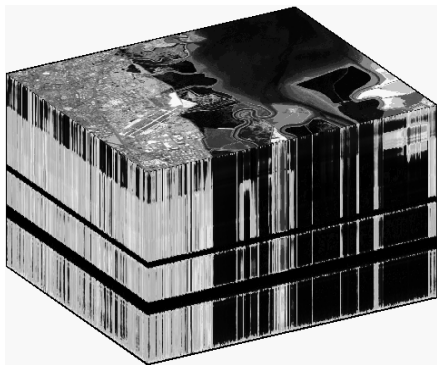


Figure 1: AVIRIS data cube Moffett Field, scene 1 (NASA, 2003)

data (e.g., in the range 140-1,000 Mb for AVIRIS images) in the form of a two dimensional image matrix each pixel consisting of many components, one for each spectral band (Figure 1).

Since hyperspectral imagery is acquired at cost and often used in critical tasks like classification (assignment of a label to every pixel) or target detection (identification of a somewhat rare instance), compression algorithms that provide lossless or near-lossless quality (for classification and detection purposes) may be required. In addition, it may be desirable to have low complexity that allows efficient on-board implementation with limited hardware. Traditional approaches to the compression of hyperspectral imagery are based on differential prediction via DPCM (Aiazzi, 2001; Abousleman, 1995; Abousleman et al., 2002), direct vector quantization (Manohar and Tilton, 2000; Ryan and Arnold, 1997; Mielikäinen and Toivanen, 2002; Pickering and Ryan, 2001) or dimensionality reduction through Principal Component Analysis.

In (Motta et al., 2003) a locally optimal design of a partitioned vector quantizer (LPVQ) for the encoding of high dimensional data is presented. The algorithm is applied to lossless, near-lossless and lossy compression of AVIRIS data. LPVQ's lossless compression, is aligned with the current state of the art. Its design and coding process, on the other hand, are computationally intensive (although highly parallelizable), while decoding is just table lookup. The asymmetrical nature of the algorithm makes it most appropriate for systems in which the codebook design does not have to be performed on-board. An inter-band linear prediction approach based on least square optimization is presented in (Mielikäinen et al., 2002). This compression method optimizes the parameters of a linear predictor with spatial and spectral support. Such optimization is performed for each sample.

Using linear prediction, least square optimization, and optimal band reordering, in

Section 2 we show how to encode efficiently the quantization indices produced by LPVQ, improving upon the baseline algorithm. We also exploit successfully the fact that spectral correlation in the original data is preserved in LPVQ indices after quantization.

In Section 3 we target the linear nature of the spectral correlation of AVIRIS data with a simple linear prediction method. The proposed method is composed by an *intra-band* predictor, similar to the one in LOCO-I (Weinberger et al., 2000), for the few bands with strong spatial correlation. The rest is encoded using a novel *inter-band* predictor. This predictor shares the same low complexity of the intra-band one, and requires buffering of at most two scan-lines from each of the previous three bands. It also uses a simplified version of the context modeling mechanism in LOCO-I that allows to match the compression performance of LPVQ. Finally we discuss experimental results and current research directions.

2 IMPROVING ENTROPY CODING OF LPVQ'S QUANTIZATION INDICES

(Motta et al., 2003) compress hyperspectral data by using a modified version of the Generalized Lloyd Algorithm to perform a dimensionality reduction of the original data. The D -dimensional input vectors are broken into L sub-vectors ($L=16$ in the reported experiments). Each sub-vector is then encoded with the 8-bit index of the closest match in the codebook generated by LPVQ, while the quantization error is encoded separately. The spatial correlation in the original data is preserved in the index files (planes), so they look very much like "natural" grayscale images. The index files are then encoded using LOCO-I.

In this section we focus on improving the compression of the quantization indices. We note that spectral dependency is still observable among index files. To take advantage of this phenomenon, we propose three methods (summarized in Table 1) two of which extend the LOCO-I/JPEG-LS predictor. They compute the prediction, based on a causal data subset (Figure 2), $\hat{x}_{i,j,k}$ of the pixel $x_{i,j,k}$ in the i -th row, j -th column of the k -th plane.

The first method in Table 1 is the one used by LOCO-I, reported here as a reference. The second, that we call INTER predictor, is similar to the one presented in (Barequet and Feder, 1999), while 3D-MED is a novel, general extension of LOCO-I to an inter-band context. These two methods share the

Table 1: linear predictors for encoding of LPVQ quantization indices.

$\hat{x}_{\text{LOCO-1}} = \text{Median}(x_{i,j-1,k}, x_{i-1,j,k}, x_{i,j-1,k} + x_{i-1,j,k} - x_{i-1,j-1,k})$
$\hat{x}_{\text{INTER}} = x_{i,j,k-1} + \text{Median}(D_{1,k}, D_{2,k}, D_{1,k} + D_{2,k} - D_{3,k})$ $D_{1,k} = x_{i,j-1,k} - x_{i,j-1,k-1}, D_{2,k} = x_{i-1,j,k} - x_{i-1,j,k-1}, D_{3,k} = x_{i-1,j-1,k} - x_{i-1,j-1,k-1}$
$\hat{x}_{\text{3D-MED}} = \text{Median}(x_{i,j-1,k}, x_{i-1,j,k}, x_{i,j,k-1}, x_{i,j-1,k} + x_{i-1,j,k} - x_{i-1,j-1,k}, x_{i,j-1,k} + x_{i,j,k-1} - x_{i,j-1,k-1}, x_{i-1,j,k} + x_{i,j,k-1} - x_{i-1,j,k-1})$
$\hat{x}_{\text{3D-LSQ}} = \sum_{j=1}^N \alpha_j x_j$

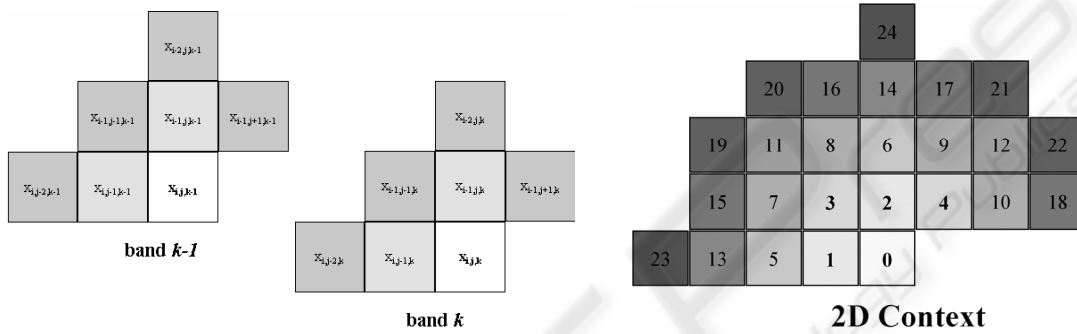


Figure 2: Prediction Template

same low complexity of the JPEG-LS standard, and hence a highly efficient implementation is possible.

The third method, 3D-LSQ, is more aggressive and computationally more expensive: given a reference plane and a 3D subset of causal data, an optimal linear predictor, in the least square sense, is determined for each sample. The prediction structure and the notation used in the following is similar to the one presented in (Brunello et al., 2002).

Two different context enumerations are defined based on the distance functions

$$d_{2D}(x_{m,n,k}, x_{p,q,k}) = \sqrt{(m-p)^2 + (n-q)^2}$$

$$d_{3D}(x_{m,n,i}, x_{p,q,j}) = \begin{cases} \sqrt{(m-p)^2 + (n-q)^2} & j=i \\ \sqrt{\frac{1}{4} + (m-p)^2 + (n-q)^2} & j \neq i \end{cases}$$

The resulting 2D and 3D context templates are showed in Figure 3.

In the following, by $x(i)$ we denote the i -th pixel in the above enumeration of the 2D context of $x_{i,j,k}$. Moreover, $x(i, j)$ denotes the j -th pixel in the 3D context of $x(i)$. The N -th order prediction of the current pixel ($x_{m,n,k} \equiv x(0,0)$), we drop the subscript and the parenthesis when referring to the current pixel) is computed as

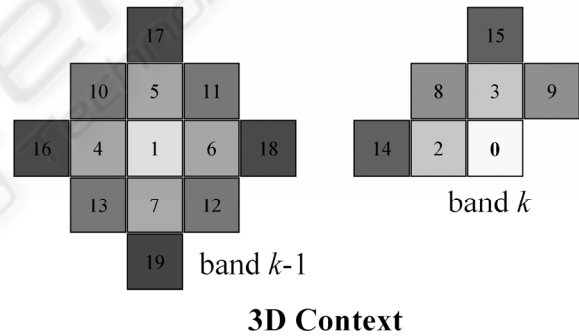


Figure 3: 2D and 3D contexts and pixel enumerations

$$\hat{x}(0,0) = \sum_{j=1}^N \alpha_j \cdot x(0, j)$$

The coefficients $\alpha_0 = [\alpha_1, \dots, \alpha_N]^t$ minimizing the energy of the prediction error

$$P = \sum_{i=1}^M (x(i,0) - \hat{x}(i,0))^2$$

are calculated using the well-known theory on optimal linear prediction. Notice that the data used in the prediction are a causal, finite sub-set of the past data and no side information needs to be sent to the decoder.

Using matrix notation, we write

$$P = (C\alpha - X)^t \cdot (C\alpha - X)$$

where,

$$\mathbf{C} = \begin{bmatrix} x(1,1) & \cdots & x(1,N) \\ \vdots & \ddots & \vdots \\ x(M,1) & \cdots & x(M,N) \end{bmatrix} \quad \mathbf{X} = \begin{bmatrix} x(1,0) \\ \vdots \\ x(M,0) \end{bmatrix}$$

By taking the derivative with respect to α and setting it to zero, the optimal predictor coefficients are the solution of the following linear system

$$(\mathbf{C}'\mathbf{C}) \cdot \alpha_0 = \mathbf{C}'\mathbf{X}$$

Once the optimal predictor coefficients for the current sample have been determined, the prediction error $\varepsilon = [x - \hat{x}]$ is encoded in the same way of the previous two methods.

3 OPTIMAL BAND ORDERING

Because each index file represents a subset of contiguous spectral bands, and because the correlation between two bands is not always inversely proportional to the distance of their wavelengths, a sequential encoding of the index files is generally suboptimal. In order to address this issue, given a function $f(i, j)$ representing the cost of encoding plane j using plane i as reference, it is possible to find the optimal plane ordering using standard graph theory results. Similar ideas could be found in (Tate, 1997; Motta and Weinberger, 2001).

Given the cost $f(i, j)$, we can define a complete weighted graph with L nodes where the weight of the edge $w_{i,j}$ is equal to $f(i, j)$. We add a fictitious node $\mathbf{0}$ connected by an edge to each node j . The weight $w_{0,j}$ represents the cost of encoding plane j without using any reference plane (e.g., using LOCO-I). The problem of optimal plane ordering is equivalent to the problem of finding the minimum spanning tree of the resulting graph (if $f(i, j)$ is not symmetrical then the graph is directed and one should compute the optimal branching rooted at $\mathbf{0}$ (Gabow et al., 1986)).

As a proof of concept, we used the first order entropy of the difference between each pair of planes as a cost function.

3.1 Context Modeling

The underlying assumption of the previous section is that the index planes generated by LPVQ look very much as “natural” images. This justifies the use of

off-shelf image-oriented techniques to encode these data. This behavior is the by-product of the lexicographical sorting of the centroids generated by LPVQ, which are “scaled/translated” version of each other. Similar behaviors are experienced in standard VQ image compression when code-vectors are arranged by increasing norm. This is not surprising because if the VQ is not rate-distortion optimal (like in most practical applications), then there must exist some inter-codeword correlation. Given the structure of LPVQ, there must be some correlation between the codeword of adjacent sub-vectors as well, hence the previous assumption is sub-optimal.

A lossless block coding of VQ code-vectors specifically designed for image compression, Address-VQ, was proposed in (Nasrabadi and Feng, 1990). Improvements were presented in (Wu et al., 1998; Gong et al., 2000), which exploited the inter-codeword correlations by means of context modeling and conditional entropy. These methods are *off-line* algorithms based on Bayes' theorem

$$P(X | X_1, X_2) = \frac{P(X_1, X_2 | X)}{P(X_1, X_2)}$$

where X is the VQ index to be coded, X_1 and X_2 causal neighbor of X).

The 3-dimensional nature of the LPVQ index planes suggests the use of a 3-D causal context. In order to assess the potentials of a Bayesian context modeling scheme, we analyzed the empirical probability $P(x_{i,j,k} | x_{i,j,k-1}, x_{i,j-1,k} - x_{i-1,j,k})$, and $P(x_{i,j,k} | x_{i,j,k-1})$ for each index plane. In general, the value of the pixel in the current plane is better predicted by the value of the corresponding pixel in the previous plane. This suggests a very simple, *on-line* scheme named PREV: define 256 entropy coders; encode $x_{i,j,k}$ using the $x_{i,j,k-1}$ -th coder (without any form of prediction).

```

proc PREV
  def EC[256], EC1 as entropy_coder

  ; encode xi,j,1 using EC1
  EncodePlane(1, EC1)

  for K = 2 to L do
    for I = 1 to ROWS do
      for J = 1 to COLS do
        Encode(xi,j,k, EC[xi,j,k-1])
      end for
    end for
  end for
end proc
    
```


Table 2: entropy coding results for LPVQ indices.

	LOCO	Sequential Coding			Optimal Band Ordering			PREV
		INTER	3D-MED	3D-LSQ	INTER	3D-MED	3D-LSQ	
Cuprite	40.44	43.44 +7.42%	44.97 +11.19%	48.82 +20.73%	47.30 +16.96%	46.11 +14.01%	50.28 +24.33%	50.52 +24.93%
Jasper Ridge	35.02	35.99 +2.77%	37.75 +7.82%	39.13 +11.76%	38.06 +8.68%	38.39 +9.64%	39.88 +13.89%	47.31 +35.09%
Low Altitude	39.10	40.61 +3.86%	42.10 +7.67%	45.96 +17.54%	44.33 +13.38%	43.15 +10.36%	47.12 +20.52%	51.93 +32.78%
LunarLake	44.45	46.30 +4.15%	48.00 +7.99%	51.22 +15.23%	49.42 +11.18%	48.91 +10.04%	52.38 +17.85%	57.72 +29.85%
Moffet Field	40.92	43.35 +5.92%	44.28 +8.19%	47.34 +15.67%	46.53 +13.70%	45.28 +10.65%	48.76 +19.14%	55.70 +36.12%
AVERAGE	39.99	41.94 +4.87%	43.42 +8.59%	46.49 +16.28%	45.13 +12.86%	44.37 +10.96%	47.68 +19.25%	52.64 +31.63%

3.2 Experimental results

Table 2 reports results in terms of compression for all schemes presented so far. The reported results for 3D-LSQ are obtained with $M=90$ and $N=9$.

As expected, when sequential coding is used, 3D-LSQ is better than the 3D-MED and the INTER predictor. Compared to the baseline LOCO-I coding, on average the improvements attained are respectively +16%, +8.54% and +4.87. When the optimal plane ordering is in use, the improvements are much higher (+19.25% for 3D-LSQ). More interestingly, the PREV prediction/compression scheme is more than 10% better than 3D-LSQ with optimal ordering, and more than 30% better than LOCO-I, used in (Motta et al., 2003). Furthermore, PREV is more than 200 times faster than 3D-LSQ on a AMD Athlon(tm) MP 1900+ based personal computer.

4 INTER-BAND LINEAR PREDICTION

Remote sensed images, like AVIRIS, show two forms of correlation: spatial (the same material tends to be present in many adjacent pixels: e.g., the water of a river) and spectral (one band can be fully or partially predicted from other bands). From our investigations emerges that the spectral correlation is generally much stronger than the spatial correlation. Furthermore, dynamic range and noise levels (instrument noise, reflection interference, aircraft movements, etc.) of AVIRIS data are much higher than those in photographic images. For these reasons the spatial predictor of LOCO-I (Table 1) tends to fail on this kind of data. Figure 4 shows the

performance in terms of bit per sample of this

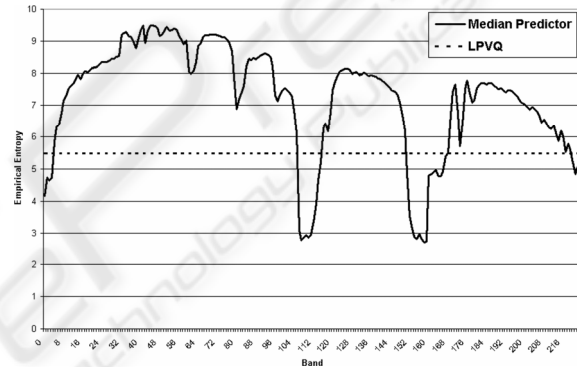


Figure 4: Empirical band entropy of the Median predictor

predictor. From our simulations it is clear that the median predictor of JPEG-LS is inefficient almost everywhere, and especially in the visible part of the spectrum that accounts for almost half of the data and it is characterized by large dynamic ranges. Nevertheless, JPEG-LS fast and efficient compression would be highly desirable to an on-board, hardware implementation.

Motivated by these considerations, we propose a novel compression method for AVIRIS data using a novel predictor for bands marked *inter-band* (IB set) and a linear predictor in the style of JPEG-LS for the rest.

This new predictor uses a simple heuristic to detect contexts in which it is likely to fail. In such cases the prediction is corrected using information about the behavior of the inter-band predictor in the previous two bands. After this prediction step, the prediction error is computed and entropy coded with a simple arithmetic coder. See Figure 5 for a formal description. After the prediction step, the prediction error is computed and entropy coded with a simple arithmetic coder.

$$\hat{x}_{i,j,k} = \begin{cases} f_{i,j,k} = x_{i,j,k} - 1 + \left\lfloor \frac{D_{1,k} + D_{2,k} + D_{3,k}}{3} \right\rfloor & k \in IB, \max_{d=1,2,3} (D_{d,k}) - \min_{d=1,2,3} (D_{d,k}) < T \\ f_{i,j,k} + \left\lfloor \frac{(x_{i,j,k-1} - f_{i,j,k-1}) + (x_{i,j,k-1} - f_{i,j,k-2})}{2} \right\rfloor & k \in IB, \max_{d=1,2,3} (D_{d,k}) - \min_{d=1,2,3} (D_{d,k}) \geq T \\ \hat{x}_{LOCO-1}(i, j, k) & k \notin IB \end{cases}$$

Figure 5: Inter-Band Linear Predictor

4.1 Least Squares Optimization

In order to set an upper bound for the achievable compression by the proposed linear prediction method and for the data under examination, we decided to implement a prediction scheme optimized for each pixel and for each band based on least squares optimization. We apply the 3D-LSQ (here named SLSQ) approach of Section 2 directly to the 224 AVIRIS bands, rather than the 16 LPVQ index planes, with $M=4$ and $N=1$.

The lossless compression results achieved by this method on AVIRIS images are, at the best of our knowledge, better than those published so far.

4.2 Experimental Results

Table 3 reports the compression ratio obtained by LP and SLSQ on the five “standard” publicly available AVIRIS images. We compare it with JPEG-LS, JPEG2000 (Taubman and Marcellin, 2001), and LPVQ. We do not report the compression results of (Mielikäinen et al., 2002) (claiming average compression ratio of 3.06:1). This is because their experimental results refer to a data sets that seems to be a subset of the one we are using and that we do not have currently available (furthermore (Mielikäinen et al., 2002) reports non-standard dimensions for AVIRIS images). LP has been applied with $IB = \Sigma - \{1 \dots 8\}$, where Σ is the set of bands, and no prediction threshold. The proposed LP method is comparable to LPVQ at a fraction of the computational cost and it is sensibly superior to the standard lossless image coders.

We also tested an extension of LP and SLSQ based on the considerations taken from Figure 4. For each scene of each cube (28 total) we checked which band was better compressed spatially (LOCO-1) rather than spectrally (LD/SLSQ). For any given band i , $i \in IB$ if and only if it has been compressed in intra mode more than 15 times over 28 (*HEU* option). A more aggressive approach (*OPT*) assumes that the encoder checks for the best method first. This requires virtually no side information (1 bit/band) and a one band look-ahead capability. For LP we also introduced a simplified version of the context modeling mechanism described in (Weinberger et al., 2000), named *LP-CTX*.

Results of improved algorithms are reported in Table 4. We report also results of *differential* JPEG-LS and *differential* JPEG2000, where by “differential” we mean that the previous band is subtracted from the current one for spectral decorrelation before applying JPEG-LS or JPEG2000. This pre-preprocessing steps improves the two standard algorithms by 40% and 53% respectively, but better compression is achieved by LP and SLSQ. As we can see, the LP-CTX with on band look-ahead improves by more than 2% the LP method, matching LPVQ compression performance at a cost of a small increase of storage requirements over baseline LP, while being 5% better than differential JPEG-LS/JPEG2000. Finally, SLSQ-OPT achieves the overall best compression. While this method needs a one band look-ahead, it has the advantage of requiring virtually no side information (1 bit/band), and since inter and intra mode could be performed in parallel, compression time is practically unchanged.

5 CONCLUSIONS

In the first part of this paper we present and analyze three linear prediction schemes for the encoding of the index planes generated by the LPVQ algorithm. The best method achieves $\approx 20\%$ improvement upon the basic schemes presented in (Motta et al., 2003). In the final subsection we show that the assumption that the index planes are comparable to “natural” images is not completely true. We also show how a very simple context modeling can achieve even better compression.

In the second part of the paper we propose a novel approach for lossless coding of AVIRIS data. It is based on an inter-band, linear predictor that, coupled with a simple entropy coder, competes with the current state of the art. The low complexity of the proposed method and its raster scan nature, makes it amenable for on-board implementations.

Since the proposed method depends loosely on the entropy coder, it would be also possible to remove the arithmetic coder and use the CCSDS standard algorithm for lossless data compression for space applications (CCSDS, 1997), whose hardware implementation is widely used on many satellites.

Table 3: Compression Results.

	JPEG-LS	JPEG2000	LPVQ	LPVQ-PREV	LP	SLSQ
Cuprite	2.09	1.91	3.13	3.18	3.03	3.15
Jaspder Ridge	2.00	1.80	2.82	2.88	2.94	3.15
Low Altitude	2.14	1.96	2.89	2.94	2.76	2.98
Lunar Lake	1.99	1.82	3.23	3.28	3.05	3.15
Moffett Field	1.91	1.78	2.94	3.00	2.88	3.14
AVERAGE	2.03	1.85	3.00	3.06	2.93	3.12

Table 4: Improvements of baseline LP and SLSQ algorithms.

	Differential JPEG-LS	Differential JPEG2000	LP-CTX			SLSQ	
			$IB = \Sigma\{1...8\}$	60%	OPT	60%	OPT
Cuprite	2.91	2.92	3.04	3.07	3.09	3.23	3.24
Jasper Ridge	2.81	2.82	2.96	2.98	3.00	3.22	3.23
Low Altitude	2.70	2.69	2.79	2.79	2.83	3.02	3.04
Lunar Lake	2.93	2.94	3.06	3.08	3.10	3.23	3.23
Moffett Field	2.84	2.83	2.93	2.94	2.96	3.20	3.21
AVERAGE	2.84	2.84	2.96	2.97	3.00	3.18	3.19

We are currently working to improve the inter-band predictor and perform a formal analysis of the remaining correlation after prediction, in order to find suitable context modeling mechanisms that will indubitably improve current performances. Near-lossless extensions are also under consideration.

REFERENCES

Abousleman, G. P. (1995). Compression of hyperspectral imagery using hybrid DPCM/DCT and entropy constrained trellis coded quantization. In Storer, J. A. and Cohn, M., editors, *Proceedings Data Compression Conference*, pages 322–331. IEEE Computer Society Press.

Abousleman, G. P., Lam, T.-T., and Karam, L. J. (2002). Robust hyperspectral image coding with channeloptimized trellis-coded quantization. *IEEE Transactions on Geoscience and Remote Sensing*, 40(4):820–830.

Aiazzi, B., Alparone, L., and Baronti, S. (2001). Nearlossless compression of 3-D optical data. *IEEE Transactions on Geoscience and Remote Sensing*, 39(11):2547–2557.

Barequet, R. and Feder, M. (1999). SICLIC: A simple intercolor lossless image coder. In Storer, J. A. and Cohn, M., editors, *Proceedings of the Data Compression Conference*, pages 501–510, Snowbird, Utha. IEEE Computer Society Press.

Brunello, D., Calvagno, G., Mian, G. A., and Rinaldo, R. (2002). Lossless video coding using optimal 3D prediction. In *Proceedings of the 9th IEEE International Conference on Image Processing (ICIP*

2002), volume 1, pages 89–92, Rochester, NY. IEEE Signal Processing Society.

CCSDS (1997). Consulting Committee for Space Data Systems, "Recommendation for space data system standards: Lossless data compression". CCSDS 121.0-B-1, Blue Book.

Gabow, H. N., Galil, Z., Spencer, T., and Tarjan, T. R. (1986). Efficient algorithms for finding minimum spanning trees in undirected and directed graphs. *Combinatorica*, 6(2):109–122.

Gong, Y., Fan, M. K. H., and Huang, C.-M. (2000). Image compression using lossless coding on VQ indexes. In Storer, J. A. and Cohn, M., editors, *Proceedings of the Data Compression Conference*, page 583, Snowbird, Utha. IEEE Computer Society Press.

Manohar, M. and Tilton, J. C. (2000). Browse level compression of AVIRIS data using vector quantization on massively parallel machine. In *Proceedings AVIRIS Airborne Geoscience Workshop*.

Mielikäinen, J., Kaarna, A., and Toivanen, P. (2002). Lossless hyperspectral image compression via linear prediction. *Proceedings of SPIE*, 4725(8):600–608.

Mielikäinen, J. and Toivanen, P. (2002). Improved vector quantization for lossless compression of AVIRIS images. In *Proceedings of the XI European Signal Processing Conference, EUSIPCO-2002*, Toulouse, France. EURASIP.

Motta, G., Rizzo, F., and Storer, J. A. (2003). On the compression of hyperspectral imagery. In Storer, J. A. and Cohn, M., editors, *Proceedings of the Data Compression Conference*, Snowbird, Utha. IEEE Computer Society Press.

Motta, G. and Weinberger, M. J. (2001). Compression of polynomial texture maps. Technical Report 143 (R.2), HP Laboratories Palo Alto.

NASA (2003). AVIRIS home page. <http://popo.jpl.nasa.gov>.

- Nasrabadi, N. M. and Feng, Y. (1990). Image compression using address-vector quantization. *IEEE Transactions on Communication*, 38:2166–2173.
- Pickering, M. and Ryan, M. (2001). Efficient spatialspectral compression of hyperspectral data. *IEEE Transactions on Geoscience and Remote Sensing*, 39(7):1536–1539.
- Ryan, M. J. and Arnold, J. F. (1997). The lossless compression of AVIRIS images by vector quantization. *IEEE Transactions on Geoscience and Remote Sensing*, 35(3):546–550.
- Tate, S. R. (1997). Band ordering in lossless compression of multispectral images. *IEEE Transactions on Computers*, 46:477–483.
- Taubman, D. and Marcellin, M. W. (2001). *Jpeg2000: Image Compression Fundamentals, Standards, and Practice*. Kluwer Academic Publishers, Boston, MA.
- Weinberger, M. J., Seroussi, G., and Sapiro, G. (1996). LOCO-I: A low complexity, context-based, lossless image compression algorithm. In Storer, J. A. and Cohn, M., editors, *Proceedings of the Data Compression Conference*, pages 140–149, Snowbird, Utha. IEEE Computer Society Press.
- Wu, X., Barthel, K. U., and Zhang, W. (1998). Piecewise 2D autoregression for predictive image coding. In *Proceedings of the International Conference on Image Processing (ICIP 1998)*, volume 3, pages 901–904. IEEE Signal Processing Society.

